Beyond Semantics: Rediscovering Spatial Awareness in Vision-Language Models

Jianing Qi[1], Jiawei Liu[1], Hao Tang[1,2], Zhigang Zhu[1,3]

[1]CUNY Graduate Center, [2]Borough of Manhattan Community College, [3]The City College of New York

jqi@gradcenter.cuny.edu, jliu9@gradcenter.cuny.edu, htang@bmcc.cuny.edu, zzhu@ccny.cuny.edu
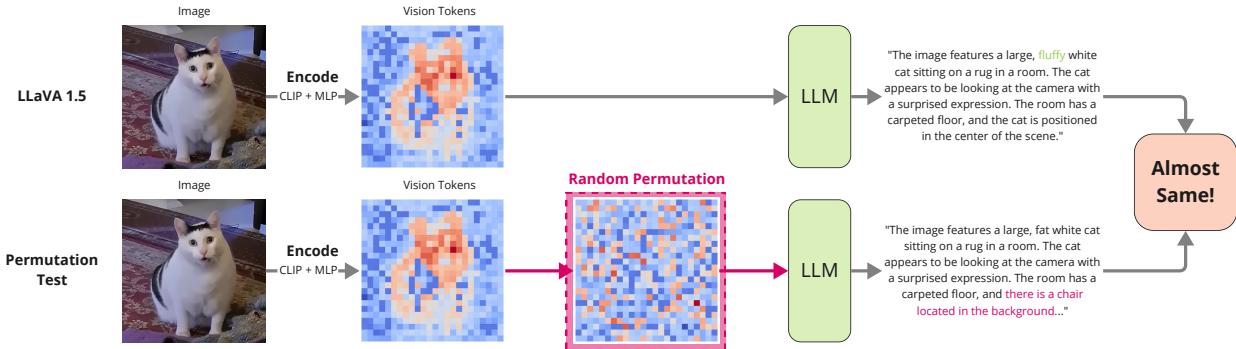
Figure 1. **Permutation Test**: Original (top) vs. randomly permuted vision tokens (bottom). Despite losing spatial ordering, the LLM accurately responds to the prompt "Describe the image," demonstrating strong robustness and a notable "bag-of-tokens" tendency. Token embeddings are visualized using cosine similarity relative to a reference token.

Abstract

Vision-Language Models (VLMs) excel at identifying and describing objects but struggle with spatial reasoning such as accurately understanding the relative positions of objects. Inspired by the dual-pathway (ventral-dorsal) model of human vision, we investigate why VLMs fail spatial tasks despite strong object recognition capabilities. Our interpretability-driven analysis reveals a critical underlying cause: vision embeddings in VLMs are treated primarily as semantic "bag-of-tokens," overshadowing subtle yet crucial positional cues due to their disproportionately large embedding norms. We validate this insight through extensive diagnostic experiments, demonstrating minimal performance impact when token orders or fine-grained spatial details are removed. Guided by these findings, we propose simple, interpretable interventions, including normalizing vision embedding norms and extracting mid-layer spatially rich features, to restore spatial awareness. Empirical results on both our synthetic data and standard benchmarks demonstrate improved spatial reasoning capabilities, highlighting the value of interpretability-informed design choices. Our study not only uncovers fundamental limitations in current VLM architectures but also provides actionable insights for enhancing structured perception of visual scenes. Website is at: user074.github.io/respatialaware/

1. Introduction

Humans process vision through two distinct pathways: the ventral stream, which identifies objects, and the dorsal stream, which encodes spatial relationships [10]. The dorsal stream, located in the parietal lobe, is essential for processing spatial relationships, allowing us to understand where objects are and how they relate to each other. Interestingly, patients with damage to the parietal lobe exhibit asymmetric visual processing: they retain the ability to recognize and describe objects but lose spatial reasoning capabilities [10].

Recent observations suggest that Vision-Language Models (VLMs) exhibit a similar asymmetry. Despite remarkable performance in object-centric (ventral) tasks such as object recognition and image captioning[2, 11, 12], VLMs systematically struggle with even fundamental spatial reasoning queries (e.g., distinguishing "left" from "right") [19, 33]. For example, when asked, "Is the apple to the left of the cup?", current state-of-the-art VLMs can accurately identify both objects, yet frequently fail to correctly infer their spatial relationship. This leads to a critical interpretability question: *Why do VLMs systematically fail at spatial reasoning even though they accurately recognize objects?*

One possible reason is the inherent treatment of visual inputs in VLMs as a "bag-of-tokens", analogous to the "bag-of-words" representation in NLP, where token order

is disregarded [13, 38]. In this kind of representation, vision embeddings lose intrinsic spatial structure, significantly limiting relational awareness. However, the underlying interpretability mechanisms behind this phenomenon remain poorly understood.

We propose that adopting the ventral-dorsal analogy provides a useful interpretability heuristic to analyze how VLMs process *what* versus *where* information. Specifically, we hypothesize that *spatial reasoning failures are exacerbated not merely by insufficient positional encoding but crucially by embedding norm suppression—the phenomenon where large embedding magnitudes overwhelm positional signals in attention mechanisms.*

To rigorously validate these hypotheses, we conduct a comprehensive interpretability-driven analysis. Building upon these interpretability insights, we propose a minimal yet interpretable solution, namely, embedding norm regulation, which is aimed at explicitly restoring 2D spatial awareness in VLMs. Through controlled experiments, we demonstrate that embedding norm normalization effectively enhances spatial reasoning without compromising semantic understanding.

In summary, our contributions include:

1. An interpretability-driven theoretical explanation for VLMs' spatial reasoning failures, rooted in embedding norm suppression.
2. Empirical interpretability evidence validating this theoretical insight through systematic permutation tests, embedding analysis, and attention visualization.
3. A simple, interpretable intervention that explicitly addresses spatial reasoning deficiencies, significantly improving performance on spatially demanding tasks.

The paper is organized as follows. After the introduction in Section 1, related work on VLMs, their intepretability and position encoding in Transformers is discussed in Section 2. Section 3 provides a diagnosis of the "Bag of Tokens" issue with token permutation and spatial compression. Detailed empirical and theoretical analyses are provided in Section 4 on spatial norm suppression. Section 5 proposes a controlled study in restoring spatial awareness of VLMs by designing a synthetic spatial benchmark. Experimental results on both synthetic and standard benchmarks are provided in Section 6. Section 7 analyzes how the combination of embedding normalization and multi-layer feature extraction influences the attention mechanisms of VLM. Section 8 discusses the findings as well as the limitations of the work, and Section 9 provides a few concluding remarks.

2. Related Work

Vision-Language Models Recent Vision-Language Models (VLMs) combine pretrained vision encoders and large language models (LLMs) to perform image understanding tasks, such as image captioning and visual question answering [1, 7, 15, 20, 23, 24, 28, 41]. Many approaches leverage pretrained visual encoders, notably CLIP [27], and subsequently introduce an adapter module to integrate vision embeddings into pretrained LLMs, such as Vicuna [6], enabling coherent textual outputs [23, 41]. While these methods achieve impressive performance in descriptive tasks, they often struggle with spatial reasoning [33, 38]. To address spatial limitations, recent efforts have focused on augmenting training datasets with extensive spatial annotations [3, 5, 32, 34]. In contrast, our approach does not rely on additional spatial labels or modifications to the original training data; instead, we introduce representation-level interventions, including embedding norm normalization and mid-layer feature extraction, which demonstrate significant improvements in VLMs' spatial reasoning capabilities.

VLM Interpretability Interpretability of Vision-Language Models has attracted increasing attention, with the aim of explaining the internal mechanisms driving their successes or failures. Neo et al. [26] show that vision tokens in LLaVA [23] have strong semantic properties. Concurrently, multiple studies have highlighted the consistent failures of VLMs to comprehend simple spatial relations such as "above," "below," "left," and "right" [4, 19, 33, 38]. These findings underscore a critical need for enhanced interpretability and robust spatial grounding in VLM architectures. Our work investigates the underlying reasons why spatial information is overshadowed in LLM, offering minimal yet effective interventions that notably strengthen the spatial reasoning ability.

Position Encoding in Transformers Positional encoding is essential in Transformer architectures to prevent degenerating into bag-of-words representations and to effectively model sequence orders [9, 35]. Initial efforts employed absolute positional encodings, later evolving into relative positional encodings [29] and, more recently, advanced mechanisms such as Rotary Positional Embeddings (RoPE) to better capture complex sequence dependencies [30]. Positional encoding has proven essential for modeling both language and visual data in Transformers [8]. Despite these developments, the specific impact of positional encodings within VLMs—where vision tokens interact with textual tokens in an LLM decoder—remains underexplored. Recent work [37] attributed hallucination issues to RoPE's long-term decay property. Complementing these insights, our work empirically and theoretically illustrates how disproportionately large embedding norms of vision tokens can overshadow positional cues, hindering spatial reasoning even when advanced positional methods like RoPE are employed.

Dataset	Original	Permutation	Difference
VQAv2	78.2	77.35	-0.85
POPE	87.3	87.10	-0.2
GQA	61.36	58.62	-2.74
CV-Bench 2D	56.59	56.26	-0.33

Table 1. Impact of random vision token permutation on spatial reasoning accuracy (%).

3. Diagnosing the Issue: Bag of Tokens

VLMs demonstrate excellent capabilities in recognizing objects within images (ventral tasks) yet consistently struggle with spatial reasoning (dorsal tasks). This disparity suggests that VLMs might neglect spatial cues in their internal representations. Open-source VLMs such as LLaVA [23] typically fuse vision embeddings with textual embeddings in transformer-based language models, relying critically on positional embeddings to encode token order. We hypothesize that in multimodal contexts, positional embeddings might become ineffective or suppressed, causing a loss of meaningful spatial structure. To investigate this, we perform two diagnostic interpretability experiments: **(1) Token Permutation Test**: If positional order significantly contributes to spatial reasoning, randomizing token order should substantially degrade model performance. We want to know how much the vision token order matters. **(2) Spatial Compression Study**: If local spatial information is crucial, drastically reducing the number of vision tokens should cause significant performance deterioration. We want to know how much VLM really uses local spatial information. Our experiments indicate that VLMs remain largely robust to these two perturbations, reinforcing the hypothesis of a "bag-of-tokens" behavior.

3.1. Token Permutation Test

In standard NLP transformers, positional embeddings are essential for maintaining token order. Similarly, if VLMs depend heavily on positional embeddings for spatial reasoning, randomizing vision token order should substantially impair spatial reasoning performance. We hypothesize that if token order carries meaningful spatial information, random shuffling should severely degrade performance.

Experiment Setup: We use LLaVA 1.5 7B from [23, 24] to conduct the test. We randomly permute vision token embeddings obtained from the vision encoder and projection layers before feeding them into the LLM, and the performance is then compared against the original unpermuted baseline. Figure 1 illustrates the experiment pipeline. We evaluate performance on datasets including VQAv2[11], POPE [21], GQA [16], and CV-Bench[32].

Result: As shown in Table 1, random token permutation leads only to minor performance drops (ranging from
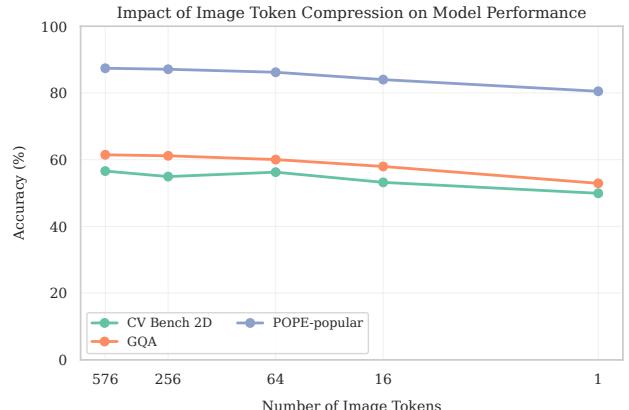

Figure 2. Performance impact of vision token compression on standard benchmarks (GQA, CV-Bench 2D, and POPE). Only minor accuracy degradation occurs, even under extreme token compression (down to a single token).

0.2% to 2.74%). This surprisingly small decline reveals that VLMs exhibit significant order-invariance, suggesting a bag of tokens tendency of VLMs. This is summarized as the following "Intepretabality Insight":

> **Interpretability Insight No. 1:** VLMs exhibit limited sensitivity to vision token order, reflecting a strong "bag-of-tokens" tendency.

3.2. Spatial Compression Study

Recent work showed VLMs focus on object semantic tokens[26]. To further probe the use of spatial information by VLMs, we progressively compress the vision tokens, effectively removing fine-grained spatial details including detailed positional and geometric relationships among image patches. If spatial details are crucial for evaluation, performance should sharply decline as spatial resolution decreases. Conversely, stable performance despite extreme compression may indicate either that *the model relies predominantly on semantic features* or that *existing benchmarks do not effectively challenge spatial reasoning capabilities*.

Experiment Setup: Using the LLaVA 1.5 7B model, we systematically reduce the number of vision tokens from the original 576 down to just 1. Models were retrained for token counts (256, 64, 16, and 1) using average pooling after the MLP projection layer. This method severely limits local spatial details while preserving some semantic content. Performance impacts are evaluated across various benchmarks.

Result: As illustrated in Figure 2, reducing the vision tokens from 576 down to just 1 for standard benchmarks results in a minor accuracy drop (-8.5% the worst case). Despite losing approximately 99.8% of spatial resolution, the model's performance remains robust. This outcome sug-

gests two interrelated explanations: first, VLMs may primarily rely on semantic cues rather than local spatial details when solving typical benchmark tasks; second, the current benchmarks themselves might not effectively test the model's capacity for detailed spatial reasoning. The limited sensitivity of these benchmarks to extreme spatial compression could reflect both model behavior and benchmark limitations. This leads us to the following insight:

> **Interpretability Insight No. 2:** For current benchmarks, VLMs can predominantly rely on "ventral" semantics rather than "dorsal" spatial cues to have a decent performance.

4. Why Does This Happen? Analysis of Embedding Norm Suppression

In earlier experiments, we observed that spatial information in VLMs tends to be minimal or overshadowed by strong global semantic signals. Here, we further investigate the underlying cause by analyzing embedding norms, specifically examining how large vision embedding magnitudes overshadow positional encodings within attention mechanisms.

4.1. Embedding Norm Analysis

Motivation Positional embeddings were initially introduced into Transformer architectures to maintain token order and avoid the "bag-of-words" effect [35]. While VLMs also utilize positional encodings during training, we hypothesize these encodings become ineffective if vision embeddings possess disproportionately large magnitudes, thus dominating positional signals during attention computations.

To investigate this hypothesis, we conduct an empirical embedding analysis using the COCO validation dataset (5000 image-text pairs) [22]. Specifically, we extract vision and text embeddings after MLP projection but before input into the language model and compute the L2 norms for each token type. Figure 3 illustrates the embedding norm distributions.

As shown in Figure 3, vision embeddings consistently have 1-2 orders of magnitudes greater than text embeddings but can reach up to 3 orders of magnitude greater at its upper range. Although directional alignment (e.g., cosine similarity) typically receives primary focus in multimodal alignment due to inner product [14, 17, 25], such large magnitude discrepancies may suppress positional signals significantly.

4.2. Theoretical Explanation

We provide a concise theoretical justification of how differences in embedding norms significantly impact the effectiveness of positional encodings in Transformer attention mechanisms. A detailed mathematical derivation is presented in the Appendix A but here is a summary.
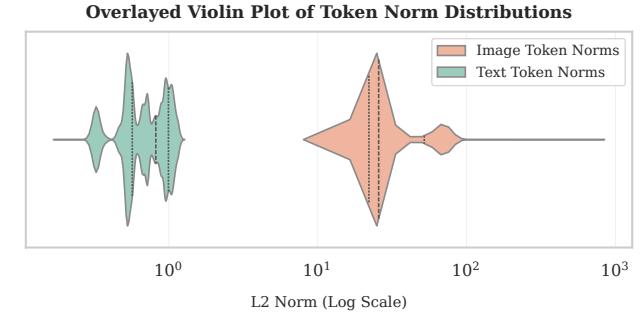

Figure 3. Distribution of L2 norms for vision and text tokens in COCO validation dataset (log scale). Vision token norms range between 10^1 and 10^3, while text token norms range between 3×10^{-1} and 10^0.

Summary of Proof (detailed derivation in Appendix A). Consider a Transformer self-attention block employing Rotary Positional Embeddings (RoPE) [31]. RoPE applies orthonormal rotations to query and key vectors with dimension d ($\mathbf{q}_i, \mathbf{k}_i \in \mathbb{R}^d$), preserving their norms. After RoPE transformation, we denote these vectors as $\mathbf{q}_i', \mathbf{k}_i' \in \mathbb{R}^d$. The attention logits between token pairs are computed via the scaled dot-product:

$$\text{logits}_{ij} = \frac{\mathbf{q}_i' \cdot \mathbf{k}_j'}{\sqrt{d}} = \frac{\|\mathbf{q}_i\| \|\mathbf{k}_j\| \cos \phi}{\sqrt{d}} \qquad (1)$$

where ϕ denotes the positional angle difference. From this expression, we observe directly that larger embedding norms increase the scale of logits. When vision embedding norms substantially exceed text embedding norms (often by an order of magnitude), vision-to-text logits dominate softmax computations, resulting in disproportionately high attention scores. To maintain coherent textual outputs aligned with the language model's training, the model implicitly learns to downscale these vision-related logits. This downscaling leads to empirically observed low attention weights for vision tokens, consistent with findings in recent studies [4]. Consequently, the positional sensitivity explicitly encoded by RoPE diminishes substantially, as lower attention weights inherently reduce the positional gradient (further detailed in Appendix A).

> **Interpretability Insight No. 3** The practical effectiveness of positional encoding mechanisms' (such as RoPE) is severely limited by embedding magnitude discrepancies between modalities.

Normalizing or rescaling embedding norms thus emerges as a crucial intervention, restoring positional sensitivity and enabling positional embeddings to meaningfully influence attention computations. This insight extends broadly to multi-modal alignment scenarios: effective alignment between pretrained models should not rely solely

on embedding similarities (such as cosine similarity) but must also carefully consider embedding norm differences. Otherwise, positional information can become suppressed, leading to minimal influence on model predictions.

5. Restoring Spatial Awareness: A Controlled Study

Our previous analyses indicated that spatial cues in VLMs are often overshadowed by strong semantic signals and disproportionately large embedding norms. To validate these findings and explore methods for enhancing spatial representations, we designed a controlled study employing two interpretability-informed strategies:

1. **Synthetic Dataset**: A carefully constructed two-dimensional (2D) spatial benchmark designed explicitly to eliminate semantic shortcuts, ensuring that spatial relationships alone drive task success.
2. **Interpretability-Informed Model Adjustments**: Targeted architectural modifications aimed at balancing positional cues and mitigating the overwhelming dominance of semantic embeddings.

Combining these controlled experimental conditions with interpretability-driven adjustments allows us to investigate the feasibility of reviving effective spatial reasoning—analogous to restoring a functional "dorsal stream"—in VLMs.

5.1. A 2D Synthetic Spatial Benchmark (2DS)

Standard image and text benchmarks often unintentionally provide semantic or contextual shortcuts, enabling models to leverage object co-occurrence or linguistic biases without genuinely understanding spatial relationships. We particularly hope to respond to the potential inadequacies in current benchmarks from our spatial compression study (Section 2). To isolate and rigorously evaluate spatial reasoning, we limit confounding factors such as real-world object frequencies and linguistic priors. Our benchmark specifically targets 2D spatial relationships directly influenced by positional embeddings.

We constructed a synthetic dataset that: (1) Ensures spatial cues are essential for correctly answering queries. (2) Isolates and systematically controls semantic aspects, enabling analysis of their contributions to spatial understanding. The dataset combines semantic attributes (color, shape, or both) with spatial properties (relative or absolute positions). We denote the **2D Synthetic Dataset as 2DS**

Example Queries including:
- "What color is at the bottom of the image?" (Color, absolute position)
- "Is the circle below the square?" (Shape, relative position)

These queries illustrate that object attributes (color, shape) serve primarily as identifiers, with positional rela-
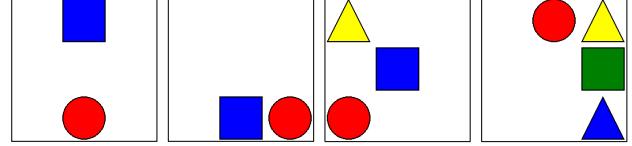

Figure 4. Illustrative scenes from our 2DS Dataset. The left two images show two object arrangements, while the right two images illustrate more complex three and four object arrangements.

tionships being crucial for correct responses.

5.1.1. Dataset Construction Details

We created meta-categories containing images with 2, 3, 4, 5, and 6 objects. Within each category, we employed the same set of objects while randomly varying their *spatial positions*. Each meta-category comprises 100 images, resulting in a total of 500 images. For every image, we systematically asked questions spanning combinations of semantic (color, shape, color and shape) *and* spatial (absolute, relative) properties, yielding 3000 total questions. Note the emphasis is on spatial relationship reasoning.

Figure 4 provides representative examples, emphasizing the simplicity of semantic attributes and the centrality of spatial relationships.

5.2. Interpretability-Informed Model Adjustments

Our interpretability analyses identified embedding norm suppression and insufficient usage of local geometric information as critical limitations to effective spatial reasoning in VLMs. Guided by these insights, we propose two straightforward and interpretable adjustments: (1) **Vision Token Normalization** and (2) **Utilizing Intermediate-Layer Features**.

Vision Token Normalization Our prior analyses revealed that vision embedding magnitudes significantly exceed those of positional embeddings, effectively suppressing positional signals during attention computations. To address this imbalance:

- **Norm Matching**: We measured the distribution of typical text embedding norms (mean ≈ 0.83, max ≈ 1.22).
- **RMS Normalization**: We applied RMS normalization [39] that is used in LLM [6] to vision encoder outputs to match them closely with textual embedding norms.

This normalization reduces the dominance of semantic signals, allowing positional cues to emerge more clearly.

Intermediate-Layer Features (Local Geometry) Current VLM architectures typically use highly aggregated, semantically-rich final-layer vision features from CLIP, which excel in semantic alignment but may lack fine-grained spatial details [36]. Recent studies suggest that intermediate layers of CLIP encoders retain richer local spatial information beneficial for VLMs [18]. Thus, we inves-
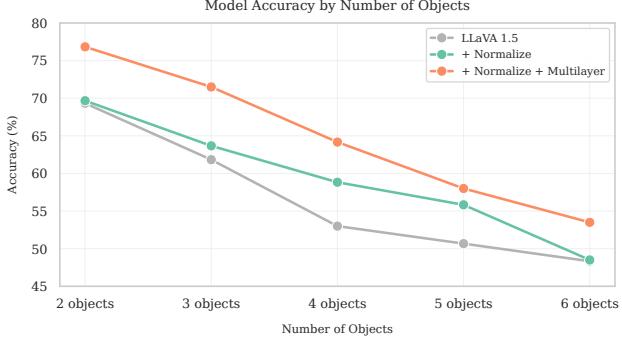
Figure 5. Accuracy comparison across varying numbers of objects. Our interpretability-informed adjustments yield consistent improvements, especially as spatial complexity increases.

tigate whether directly incorporating earlier spatial features improves spatial reasoning.

Specifically, we extracted features from intermediate vision encoder layers (12, 16, 20, and 24), inherently containing more detailed spatial information reminiscent of the dorsal-stream processing pathway. These mid-layer features explicitly encode fine-grained local spatial information, potentially crucial for accurately answering purely spatial queries in our synthetic dataset.

However, an interpretability-informed ablation study (Section 7.2) reveals a semantic-spatial trade-off: while intermediate features significantly boost purely spatial task performance, they might also reduce the LLM's incentive to develop explicit positional sensitivity within its attention mechanism.

6. Experiments

We now evaluate the effectiveness of our interpretability-informed interventions, namely vision embedding normalization and intermediate-layer feature extraction, in enhancing spatial reasoning in VLMs. Our experiments cover results on both a controlled synthetic spatial benchmark and several standard vision-language benchmarks.

6.1. Experimental Setup

We use LLaVA 1.5 (7B) [23] as our baseline model, which is chosen for its open-source availability and transparent training details. We replicate LLaVA 1.5's exact two-stage training process and dataset usage for fair comparison. Based on the interpretability insights discussed earlier, we evaluate two proposed variants:

- **+ Normalize**: Vision embeddings normalized according to the procedure detailed in Section 5.2.
- **+ Normalize + Multilayer**: Normalized vision embeddings augmented with intermediate-layer features to retain fine-grained spatial information (Section 5.2).
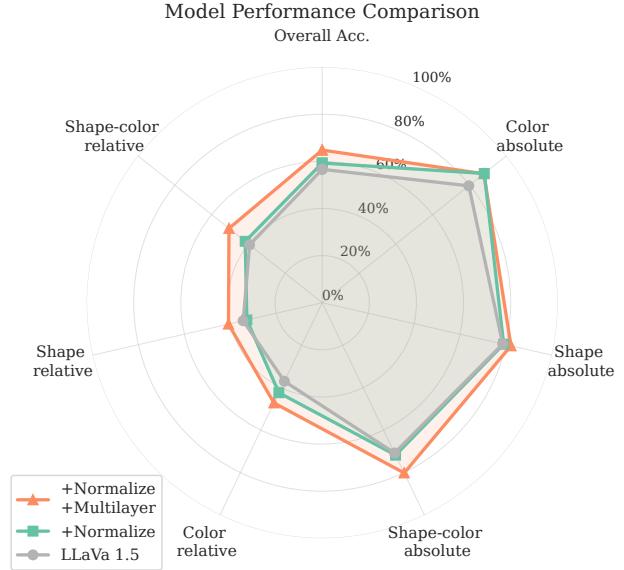

Figure 6. Accuracy comparison across different categories of 2DS dataset. We see consistent improvements across categories.

Category	LLaVA 1.5	+ Normalize	+ Normalize + Multilayer
Color_abs. ↑	79.60	**88.00** (+8.40)	87.80 (+8.20)
Color_rel. ↑	37.00	42.40 (+5.40)	**47.20** (+10.20)
Shape_abs. ↑	78.60	79.00 (+0.40)	**82.20** (+3.60)
Shape_rel. ↑	34.40	32.80 (-1.60)	**40.80** (+6.40)
Shape_color_abs. ↑	70.80	71.80 (+1.00)	**80.20** (+9.40)
Shape_color_rel. ↑	39.40	41.80 (+2.40)	**50.60** (+11.20)
Overall Acc. ↑	56.63	59.30 (+2.67)	**64.80** (+8.17)

Table 2. Spatial reasoning accuracy (%) across 2DS categories. ↑ indicates higher is better. Values in parentheses show difference from LLaVA 1.5 baseline.

6.2. Results on Synthetic Dataset

Table 2 summarizes accuracy across distinct spatial query categories, and Figure 6 illustrates performance across varying numbers of objects, clearly highlighting the effectiveness of our interventions.

Vision Embedding Normalization: Normalization alone improves overall accuracy from 56.63% to 59.30%, strongly supporting our interpretability insight that balancing embedding norms significantly enhances spatial information utilization. Notably, improvements are particularly pronounced in color-related spatial relationship queries.

Normalization + Intermediate-layer Features: This approach achieves the highest overall accuracy (64.80%, +8.17% improvement over baseline), underscoring the importance of explicitly incorporating local spatial details. This method substantially enhances accuracy, especially in shape and color combined relative position queries.
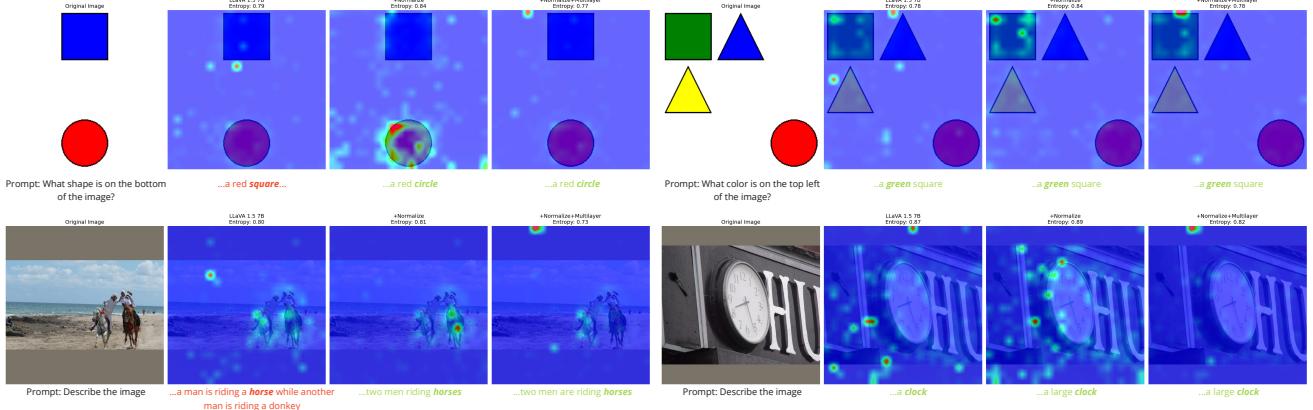
6

Figure 7. Visualization of self-attention patterns. We overlay the attention map on top of the image. The question for the model is under each row. We use the first target word of the response for attention map, for example the attention map is based on 'square' and 'circle' for top left rows. Entropy values are on top of each image. Red answers are wrong. Green answers are correct. Each image has entropy on top: lower means more concentrated higher means more diffused

Both methods consistently outperform the original LLaVA 1.5 model, particularly as spatial complexity (the number of objects) increases (Figure 5), validating our hypothesis about the critical roles of embedding normalization and local spatial detail preservation.

6.3. Results on Standard Benchmarks

Category	LLaVA 1.5	+ Normalize	+ Normalize + Multilayer
VQAv2 ↑	78.20	78.76 (+0.56)	**79.17** (+0.97)
POPE ↑	87.30	87.30 (0.00)	**87.70** (+0.40)
GQA ↑	61.46	62.04 (+0.58)	**62.52** (+1.05)
CV-Bench2D ↑	56.59	**59.91** (+3.32)	58.69 (+2.10)

Table 3. Performance (accuracy %) on standard vision-language benchmarks. ↑ indicates higher is better. Values in parentheses show difference from LLaVA 1.5 baseline.

To assess generalization, we evaluate our methods on established benchmarks (Table 3) that are used in recent works [23, 24, 32, 41].

Both interpretability-informed interventions yield moderate yet consistent improvements. Normalization and Multilayer Normalization consistently achieves small but meaningful gains (up to 3.32%), confirming that improved spatial representation benefits overall reasoning without sacrificing semantic capabilities. Notably, normalization shows more pronounced gains in the CV-Bench 2D dataset, particularly for spatial relationship tasks.

7. Analysis

To deepen our interpretability-driven understanding, we analyzed how the combination of **embedding normalization** and **earlier-layer feature extraction** influences the attention mechanisms of VLMs.

7.1. Attention Visualization

We visualized the self-attention patterns from LLM to interpret the effects of each modification on spatial reasoning. Figure 7 provides representative attention maps across four illustrative queries. Each query compares three scenarios: the baseline (Original LLaVA 1.5), normalized embeddings, and normalized embeddings combined with multilayer features. We visualized the first text token of the target object in the answer, which are bold and italic words in Figure 7. More examples are in Appendix C.

Baseline (Original LLaVA 1.5): The baseline model shows diffuse and scattered attention patterns, possibly influenced by large-magnitude vision embeddings that overshadow positional cues. This diffuseness makes it difficult for the model to clearly focus on relevant spatial tokens, leading to suboptimal spatial reasoning.

Embedding Normalization: Embedding normalization leads to distinct and focused attention distributions, significantly increasing attention on relevant spatial tokens. Interestingly, this variant exhibits broader coverage of the attention map, suggesting that the model actively utilizes positional embeddings to locate informative spatial regions. The improved spatial focus directly contributes to enhanced performance in spatial reasoning tasks.

Embedding Normalization + Multilayer Features: Interestingly, the multilayer feature variant produces sparser, more selective attention distributions with lower attention magnitudes, similar visually to the original model but fundamentally different in effectiveness. Despite lower peak attention, this variant consistently performs better across

7

Vision Token Attention Entropy	LLaVA 1.5	+ Normalize	+ Normalize + Multilayer
2DS ↓	0.76	0.90	**0.72**
COCO Val ↓	0.81	0.89	**0.72**
CV-Bench2D ↓	0.80	0.90	**0.72**

Table 4. Average attention entropy over different datasets. Lower entropy indicates more selective attention.

most spatial tasks. We hypothesize that intermediate-layer vision embeddings inherently carry sufficient local spatial information, thus significantly reducing the need for explicit positional encoding at the LLM stage. Consequently, the model selectively focuses attention on regions already identified as informative by intermediate-layer embeddings without the need to check other regions.

7.2. Interpreting Attention Patterns and Performance

To quantitatively interpret these observations, we computed the normalized attention entropy (Table 4). We average all text tokens' attention over the vision tokens to compute the entropy. Lower entropy indicates more targeted attention distributions, and high scores mean more diffused attention distributions. More examples are in Appendix C.

The normalized embeddings exhibit higher entropy compared to the baseline, reflecting a broader and more uniform exploration of spatial regions, yet with a clear focus on the target object. This suggests that embedding normalization encourages the LLM to explicitly explore multiple spatial positions to extract positional information. In contrast, the multilayer normalized variant demonstrates the lowest entropy, underscoring the model's confidence in selectively attending to a few precise spatial regions. This observation supports our hypothesis that intermediate-layer embeddings inherently encode robust spatial details, enabling the model to rely less on explicit attention-based positional signals to look at vision tokens. In addition, it suggests that the improvements of the Normalize and Multilayer Normalize are two different mechanisms: the former is based on LLM attention, and the later is based on vision encoder spatial information.

> **Interpretability Insight No.4.** This analysis underscores a fundamental interpretability trade-off: richer spatial information embedded earlier in the model pipeline reduces the dependence on explicit positional encoding effect at later stages. Consequently, LLM attention becomes sparser yet highly targeted, reflecting enhanced target in spatial information rather than a failure to attend effectively.

Providing early-layer features from vision encoders potentially offers a shortcut for LLMs to directly leverage spatial cues without extensive positional encoding training. Future research should explore strategies to optimally balance intermediate-layer spatial detail and positional encodings.

8. Discussion

Our experiments reveal that spatial reasoning in VLMs is often overshadowed by strong semantic cues and disproportionately large vision token norms. Normalizing embedding magnitudes and incorporating intermediate-layer vision features partially restore a dorsal-stream-like spatial awareness. The most pronounced improvements occur in our synthetic dataset, explicitly designed to emphasize spatial over semantic shortcuts.

This analysis represents an initial step toward deeper interpretability in VLMs. It highlights that not only dataset design but also detailed model analysis is crucial. Careful alignment of multi-modal representations, especially when leveraging pretrained models, is essential. Our findings provide actionable insights for achieving more effective modality alignment in future research.

Limitations Despite the promising results, our approach has several limitations: First, the proposed model adjustments are intentionally simple to illustrate our interpretability insights. The current normalization method is a brute-force matching to text embedding norms, and it can be overly simplistic. Second, there exists a fundamental trade-off regarding where spatial information is encoded. Normalization pushes LLMs to utilize positional signals explicitly, while multilayer normalization leverages inherent spatial details from vision encoders Finally, current evaluations focus primarily on 2D spatial reasoning tasks. In 3D, the larger magnitude might be more beneficial.

Future Directions. Future work should expand spatial benchmarks to robustly evaluate complex 3D reasoning and explore refined normalization methods that preserve semantic information while still promoting spatial awareness. Additionally, architectural modifications explicitly designed for balanced semantic and spatial reasoning could further advance VLM interpretability and effectiveness.

9. Conclusion

Through systematic diagnosis and interpretability-driven analysis of VLMs, we propose minimal yet impactful interventions that restore dorsal-stream-like spatial reasoning capabilities. Our insights highlight the critical role of embedding norms and layer-specific features, providing a clear interpretability pathway for future model improvements. As research increasingly seeks models capable of accurately understanding not only *what* objects exist but precisely *where* they are, our contributions lay a foundation for more spatially intelligent, interpretable, and effective VLMs.

References

[1] Jean-Baptiste Alayrac, Jeff Donahue, Pauline Luc, Antoine Miech, Iain Barr, Yana Hasson, Karel Lenc, Arthur Mensch, Katherine Millican, Malcolm Reynolds, Roman Ring, Eliza Rutherford, Serkan Cabi, Tengda Han, Zhitao Gong, Sina Samangooei, Marianne Monteiro, Jacob L Menick, Sebastian Borgeaud, Andy Brock, Aida Nematzadeh, Sahand Sharifzadeh, Mikoł aj Bińkowski, Ricardo Barreira, Oriol Vinyals, Andrew Zisserman, and Karén Simonyan. Flamingo: a visual language model for few-shot learning. In *Advances in Neural Information Processing Systems*, pages 23716–23736. Curran Associates, Inc., 2022. 2

[2] Stanislaw Antol, Aishwarya Agrawal, Jiasen Lu, Margaret Mitchell, Dhruv Batra, C. Lawrence Zitnick, and Devi Parikh. Vqa: Visual question answering. In *Proceedings of the IEEE International Conference on Computer Vision (ICCV)*, 2015. 1

[3] Boyuan Chen, Zhuo Xu, Sean Kirmani, Brain Ichter, Dorsa Sadigh, Leonidas Guibas, and Fei Xia. Spatialvlm: Endowing vision-language models with spatial reasoning capabilities. In *Proceedings of the IEEE/CVF Conference on Computer Vision and Pattern Recognition (CVPR)*, pages 14455–14465, 2024. 2

[4] Shiqi Chen, Tongyao Zhu, Ruochen Zhou, Siyang Gao, Juan Carlos Niebles, Mor Geva, Junxian He, Jiajun Wu, and Manling Li. Adaptvis: Spatial understanding in vision-language models requires adaptive attention, 2024. 2, 4, 1

[5] An-Chieh Cheng, Hongxu Yin, Yang Fu, Qiushan Guo, Ruihan Yang, Jan Kautz, Xiaolong Wang, and Sifei Liu. SpatialRGPT: Grounded spatial reasoning in vision-language models. In *The Thirty-eighth Annual Conference on Neural Information Processing Systems*, 2024. 2

[6] Wei-Lin Chiang, Zhuohan Li, Zi Lin, Ying Sheng, Zhanghao Wu, Hao Zhang, Lianmin Zheng, Siyuan Zhuang, Yonghao Zhuang, Joseph E. Gonzalez, Ion Stoica, and Eric P. Xing. Vicuna: An open-source chatbot impressing gpt-4 with 90%* chatgpt quality, 2023. 2, 5

[7] Yang Ding, Jing Yu, Bang Liu, Yue Hu, Mingxin Cui, and Qi Wu. Mukea: Multimodal knowledge extraction and accumulation for knowledge-based visual question answering. In *Proceedings of the IEEE/CVF Conference on Computer Vision and Pattern Recognition (CVPR)*, pages 5089–5098, 2022. 2

[8] Alexey Dosovitskiy, Lucas Beyer, Alexander Kolesnikov, Dirk Weissenborn, Xiaohua Zhai, Thomas Unterthiner, Mostafa Dehghani, Matthias Minderer, Georg Heigold, Sylvain Gelly, Jakob Uszkoreit, and Neil Houlsby. An image is worth 16x16 words: Transformers for image recognition at scale. In *International Conference on Learning Representations*, 2021. 2

[9] Philipp Dufter, Martin Schmitt, and Hinrich Schütze. Position information in transformers: An overview. *Computational Linguistics*, 48(3):733–763, 2022. 2

[10] Melvyn A. Goodale and A.David Milner. Separate visual pathways for perception and action. *Trends in Neurosciences*, 15(1):20–25, 1992. 1

[11] Yash Goyal, Tejas Khot, Douglas Summers-Stay, Dhruv Batra, and Devi Parikh. Making the V in VQA matter: Elevating the role of image understanding in Visual Question Answering. In *Conference on Computer Vision and Pattern Recognition (CVPR)*, 2017. 1, 3

[12] Danna Gurari, Qing Li, Abigale J. Stangl, Anhong Guo, Chi Lin, Kristen Grauman, Jiebo Luo, and Jeffrey P. Bigham. Vizwiz grand challenge: Answering visual questions from blind people. In *2018 IEEE/CVF Conference on Computer Vision and Pattern Recognition*, pages 3608–3617, 2018. 1

[13] Roei Herzig, Alon Mendelson, Leonid Karlinsky, Assaf Arbelle, Rogerio Feris, Trevor Darrell, and Amir Globerson. Incorporating structured representations into pretrained vision \& language models using scene graphs. In *The 2023 Conference on Empirical Methods in Natural Language Processing*, 2023. 2

[14] Jack Hessel, Ari Holtzman, Maxwell Forbes, Ronan Le Bras, and Yejin Choi. CLIPScore: A reference-free evaluation metric for image captioning. In *Proceedings of the 2021 Conference on Empirical Methods in Natural Language Processing*, pages 7514–7528, Online and Punta Cana, Dominican Republic, 2021. Association for Computational Linguistics. 4

[15] Xiaowei Hu, Zhe Gan, Jianfeng Wang, Zhengyuan Yang, Zicheng Liu, Yumao Lu, and Lijuan Wang. Scaling up vision-language pre-training for image captioning. In *Proceedings of the IEEE/CVF Conference on Computer Vision and Pattern Recognition (CVPR)*, pages 17980–17989, 2022. 2

[16] Drew A. Hudson and Christopher D. Manning. Gqa: A new dataset for real-world visual reasoning and compositional question answering, 2019. 3

[17] Minyoung Huh, Brian Cheung, Tongzhou Wang, and Phillip Isola. Position: The platonic representation hypothesis. In *Proceedings of the 41st International Conference on Machine Learning*, pages 20617–20642. PMLR, 2024. 4

[18] Dongsheng Jiang, Yuchen Liu, Songlin Liu, Jin'e Zhao, Hao Zhang, Zhen Gao, Xiaopeng Zhang, Jin Li, and Hongkai Xiong. From clip to dino: Visual encoders shout in multimodal large language models, 2024. 5

[19] Amita Kamath, Jack Hessel, and Kai-Wei Chang. What's "up" with vision-language models? investigating their struggle with spatial reasoning. In *The 2023 Conference on Empirical Methods in Natural Language Processing*, 2023. 1, 2

[20] Junnan Li, Dongxu Li, Silvio Savarese, and Steven Hoi. BLIP-2: Bootstrapping language-image pre-training with frozen image encoders and large language models. In *Proceedings of the 40th International Conference on Machine Learning*, pages 19730–19742. PMLR, 2023. 2

[21] Yifan Li, Yifan Du, Kun Zhou, Jinpeng Wang, Wayne Xin Zhao, and Ji-Rong Wen. Evaluating object hallucination in large vision-language models, 2023. 3

[22] Tsung-Yi Lin, Michael Maire, Serge Belongie, Lubomir Bourdev, Ross Girshick, James Hays, Pietro Perona, Deva Ramanan, C. Lawrence Zitnick, and Piotr Dollár. Microsoft coco: Common objects in context, 2015. 4

[23] Haotian Liu, Chunyuan Li, Qingyang Wu, and Yong Jae Lee. Visual instruction tuning. In *Advances in Neural Information Processing Systems*, pages 34892–34916. Curran Associates, Inc., 2023. 2, 3, 6, 7

[24] Haotian Liu, Chunyuan Li, Yuheng Li, and Yong Jae Lee. Improved baselines with visual instruction tuning. In *Proceedings of the IEEE/CVF Conference on Computer Vision and Pattern Recognition (CVPR)*, pages 26296–26306, 2024. 2, 3, 7

[25] Mayug Maniparambil, Raiymbek Akshulakov, Yasser Abdelaziz Dahou Djilali, Mohamed EI Amine Seddik, Sanath Narayan, Karttikeya Mangalam, and Noel E. O'Connor. Do vision and language encoders represent the world similarly? In *2024 IEEE/CVF Conference on Computer Vision and Pattern Recognition (CVPR)*, pages 14334–14343, 2024. 4

[26] Clement Neo, Luke Ong, Philip Torr, Mor Geva, David Krueger, and Fazl Barez. Towards interpreting visual information processing in vision-language models. In *The Thirteenth International Conference on Learning Representations*, 2025. 2, 3

[27] Alec Radford, Jong Wook Kim, Chris Hallacy, Aditya Ramesh, Gabriel Goh, Sandhini Agarwal, Girish Sastry, Amanda Askell, Pamela Mishkin, Jack Clark, Gretchen Krueger, and Ilya Sutskever. Learning transferable visual models from natural language supervision, 2021. 2

[28] Zhenwei Shao, Zhou Yu, Meng Wang, and Jun Yu. Prompting large language models with answer heuristics for knowledge-based visual question answering. In *Proceedings of the IEEE/CVF Conference on Computer Vision and Pattern Recognition (CVPR)*, pages 14974–14983, 2023. 2

[29] Peter Shaw, Jakob Uszkoreit, and Ashish Vaswani. Self-attention with relative position representations, 2018. 2

[30] Jianlin Su, Yu Lu, Shengfeng Pan, Ahmed Murtadha, Bo Wen, and Yunfeng Liu. Roformer: Enhanced transformer with rotary position embedding, 2023. 2, 1

[31] Jianlin Su, Murtadha Ahmed, Yu Lu, Shengfeng Pan, Wen Bo, and Yunfeng Liu. Roformer: Enhanced transformer with rotary position embedding. *Neurocomputing*, 568:127063, 2024. 4

[32] Shengbang Tong, Ellis L Brown II, Penghao Wu, Sanghyun Woo, ADITHYA JAIRAM IYER, Sai Charitha Akula, Shusheng Yang, Jihan Yang, Manoj Middepogu, Ziteng Wang, Xichen Pan, Rob Fergus, Yann LeCun, and Saining Xie. Cambrian-1: A fully open, vision-centric exploration of multimodal LLMs. In *The Thirty-eighth Annual Conference on Neural Information Processing Systems*, 2024. 2, 3, 7

[33] Shengbang Tong, Zhuang Liu, Yuexiang Zhai, Yi Ma, Yann LeCun, and Saining Xie. Eyes wide shut? exploring the visual shortcomings of multimodal llms, 2024. 1, 2

[34] Ameni Trabelsi, Maria Zontak, Yiming Qian, Brian Jackson, Suleiman Khan, and Umit Batur. What matters when building vision language models for product image analysis? 2025. 2

[35] Ashish Vaswani, Noam Shazeer, Niki Parmar, Jakob Uszkoreit, Llion Jones, Aidan N Gomez, Ł ukasz Kaiser, and Illia Polosukhin. Attention is all you need. In *Advances in Neural Information Processing Systems*. Curran Associates, Inc., 2017. 2, 4, 1

[36] Guangzhi Wang, Yixiao Ge, Xiaohan Ding, Mohan Kankanhalli, and Ying Shan. What makes for good visual tokenizers for large language models?, 2023. 5

[37] Yun Xing, Yiheng Li, Ivan Laptev, and Shijian Lu. Mitigating object hallucination via concentric causal attention. In *The Thirty-eighth Annual Conference on Neural Information Processing Systems*, 2024. 2

[38] Mert Yuksekgonul, Federico Bianchi, Pratyusha Kalluri, Dan Jurafsky, and James Zou. When and why vision-language models behave like bags-of-words, and what to do about it? In *The Eleventh International Conference on Learning Representations*, 2023. 2

[39] Biao Zhang and Rico Sennrich. Root mean square layer normalization. In *Advances in Neural Information Processing Systems*. Curran Associates, Inc., 2019. 5

[40] Jingyang Zhang. Vlm-visualizer. https://github.com/zjysteven/VLM-Visualizer, 2024. 2

[41] Deyao Zhu, Jun Chen, Xiaoqian Shen, Xiang Li, and Mohamed Elhoseiny. MiniGPT-4: Enhancing vision-language understanding with advanced large language models. In *The Twelfth International Conference on Learning Representations*, 2024. 2, 7

Beyond Semantics: Rediscovering Spatial Awareness in Vision-Language Models

Supplementary Material

A. Theoretical Analysis of Large-Norm Effects on RoPE

Problem Setup

Consider a Transformer attention mechanism [35] employing Rotary Position Embeddings (RoPE)[30]. Each token i generates a query $\mathbf{q}_i \in \mathbb{R}^d$ and a key $\mathbf{k}_i \in \mathbb{R}^d$. RoPE applies a position-dependent rotation $R(\cdot)$, transforming these vectors as follows:

$$\mathbf{q}'_i = R(\mathbf{q}_i), \quad \mathbf{k}'_i = R(\mathbf{k}_i).$$

For simplicity, assume $R(\cdot)$ preserves norms (this is standard for RoPE since it only rotates but does not change norm):

$$\|\mathbf{q}'_i\| = \|\mathbf{q}_i\|, \quad \|\mathbf{k}'_i\| = \|\mathbf{k}_i\|.$$

The attention logits are computed using scaled dot-product attention:

$$\text{logit}_{\text{txt,vis}} = \frac{\mathbf{q}'_i \cdot \mathbf{k}'_j}{\sqrt{d}}$$

1. Effects of Large Embedding Norms on Attention Weights

When vision embedding input into LLM directly without model parameter adjustments, we can generally assume the Query and Key of the vision embedding will scale accordingly. Consider two sets of embeddings: vision embeddings $\mathbf{q}_{\text{vis}}$, $\mathbf{k}_{\text{vis}}$ and text embeddings $\mathbf{q}_{\text{txt}}$, $\mathbf{k}_{\text{txt}}$. Empirically, we observed (as illustrated in the Section 4.1) that vision embeddings typically have substantially larger norms than text embeddings:

$$\|\mathbf{q}_{\text{vis}}\| \approx M\|\mathbf{q}_{\text{txt}}\|, \|\mathbf{k}_{\text{vis}}\| \approx M\|\mathbf{k}_{\text{txt}}\|, \quad M \gg 1.$$

Empirically, from our study M can reach to the level of 10^1 to 10^2 range. Then based on Cauchy-Schwarz inequality we can simply drive following approximations for the attention logits for vision-to-text interactions:

$$\text{logit}_{\text{txt,vis}} = \frac{\mathbf{q}'_{\text{txt}} \cdot \mathbf{k}'_{\text{vis}}}{\sqrt{d}} \leq \frac{\|\mathbf{q}'_{\text{txt}}\|\|\mathbf{k}'_{\text{vis}}\|}{\sqrt{d}} \approx \frac{M\|\mathbf{q}'_{\text{txt}}\|\|\mathbf{k}'_{\text{txt}}\|}{\sqrt{d}}$$

Similarly, for text-to-text interactions:

$$\text{logit}_{\text{txt,txt}} \approx \frac{\|\mathbf{q}'_{\text{txt}}\|\|\mathbf{k}'_{\text{txt}}\|}{\sqrt{d}}$$

Given the scale difference ($M \gg 1$), typically we can see that:

$$\text{logit}_{\text{txt,vis}} \approx \frac{M\|\mathbf{q}'_{\text{txt}}\|\|\mathbf{k}'_{\text{txt}}\|}{\sqrt{d}} \gg \frac{\|\mathbf{q}'_{\text{txt}}\|\|\mathbf{k}'_{\text{txt}}\|}{\sqrt{d}} \approx \text{logit}_{\text{txt,txt}}$$

It would follow that the softmax attention weights from vision tokens towards text tokens become disproportionately large if not adjusted:

$$\alpha_{\text{txt,vis}} = softmax(\frac{\mathbf{q}_{\text{txt}} \cdot \mathbf{k}_{\text{vis}}}{\sqrt{d}}) = \frac{\exp(\text{logit}_{\text{txt,vis}})}{\sum_j \exp(\text{logit}_{\text{txt},j})} \quad (2)$$

$$= \frac{\exp(\text{logit}_{\text{txt,vis}})}{\sum_{j_{vis}} \exp(\text{logit}_{\text{txt},j_{vis}}) + \sum_{j_{txt}} \exp(\text{logit}_{\text{txt},j_{txt}})} \quad (3)$$

It is easy to see that the terms are dominated by the large M discrepancies between the vision and text embeddings. However, practical model training implicitly enforces coherence conditioned primarily on textual tokens, forcing the model to scale down vision-query logits significantly. This downscaling results in empirically observed low attention weights for vision tokens. [4] observed the attention score of vision tokens are way much smaller compared to the attention weights of text tokens based on the score of the text token, and the score of vision token for most of layers are in $[0, 0.2]$ range while text tokens are in $[0.8, 1]$ range. It is reasonable to believe the model learned to scale down $\text{logit}_{\text{txt,vis}}$ significantly to balance out the large norm.

2. Impact on RoPE and Positional Encoding

The attention weight for token j given query token i is defined by the softmax function:

$$\alpha_{\text{txt,vis}} = \frac{\exp(\text{logit}_{\text{txt,vis}})}{\sum_k \exp(\text{logit}_{\text{txt},k})}$$

We analyze how sensitively the attention weight $\alpha_{\text{txt,vis}}$ varies with respect to the positional angle ϕ, introduced by the Rotary Position Embedding (RoPE). This sensitivity is given by the derivative:

$$\frac{\partial \alpha_{\text{txt,vis}}}{\partial \phi} = \frac{\partial}{\partial \phi} \left(\frac{\exp(\text{logit}_{\text{txt,vis}})}{\sum_k \exp(\text{logit}_{\text{txt},k})} \right)$$

Expanding this derivative explicitly with the quotient rule, we can denote $\exp(\text{logit}_{\text{txt,vis}})$ as u and $\sum_k \exp(\text{logit}_{\text{txt},k})$ as v, then we have:

$$\frac{\partial \alpha_{\text{txt,vis}}}{\partial \phi} = \frac{vu' - uv'}{v^2}$$

then simplifying the exponential derivatives and factoring out $\alpha_{\text{txt,vis}}$, we simplify it to:

$$\frac{\partial \alpha_{\text{txt,vis}}}{\partial \phi} = \alpha_{\text{txt,vis}} \left(\frac{\partial \text{logit}_{\text{txt,vis}}}{\partial \phi} - \sum_k \alpha_{\text{txt},k} \frac{\partial \text{logit}_{\text{txt},k}}{\partial \phi} \right)$$

Key Insight From this expression, we observe that the positional sensitivity (derivative) of the attention weight explicitly depends on the attention weight itself ($\alpha_{\text{txt,vis}}$). Therefore, when the attention weight $\alpha_{\text{txt,vis}}$ is small (as in the case of vision tokens after significant normalization), the derivative with respect to positional angle ϕ is correspondingly reduced, diminishing positional distinctiveness.

> **Mathematical Justification:**
> The derivative of attention weights (softmax) w.r.t. positional angle ϕ is directly proportional to the attention weight itself:
>
> $$\frac{\partial \alpha_{\text{txt,vis}}}{\partial \phi} = \alpha_{\text{txt,vis}} \left(\frac{\partial \text{logit}_{\text{txt,vis}}}{\partial \phi} - \sum_k \alpha_{\text{txt},k} \frac{\partial \text{logit}_{\text{txt},k}}{\partial \phi} \right)$$
>
> Thus, lower attention weights inherently reduce positional sensitivity, explaining why downscaled vision embeddings exhibit diminished positional distinctiveness after normalization.

B. Training Details

We follow the training recipe described in LLaVA 1.5 7B [23], consisting of two stages: pretraining and instruction tuning. All experiments utilize 8 Nvidia A100 GPUs. Learning rates for each training stage are detailed in Table 5, with all other hyperparameters and datasets identical to [23].

Model	Pre-train	Finetune
LLaVA 1.5 7B	1e-3	2e-5
+Normalize	1e-3	2e-5
+Normalize+Multilayer	1e-3	2e-5

Table 5. Learning rate of training

C. Attention Entropy

We adapt the visualization method from [40] to analyze the LLM attention specifically on vision tokens. Attention maps correspond to particular, meaningful text tokens, as labeled above each image in Figure 8. This is a more refined version compared to average text tokens. Notably, we observe consistently lower entropy in the multilayer-normalized models.
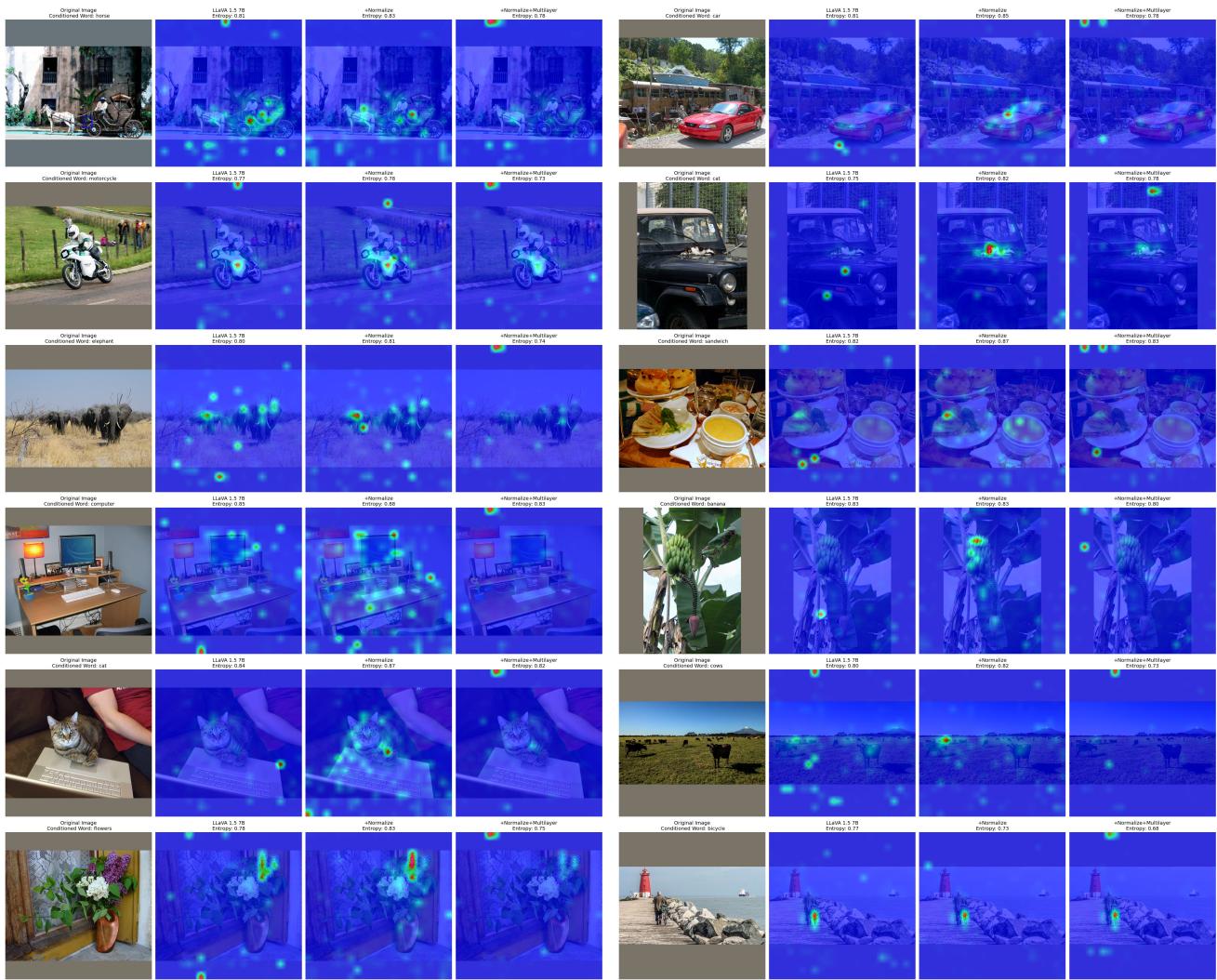
Figure 8. More visualizations